

3522

NACA TN 3231



NATIONAL ADVISORY COMMITTEE FOR AERONAUTICS

TECHNICAL NOTE 3231

BENDING TESTS ON BOX BEAMS HAVING SOLID- AND
OPEN-CONSTRUCTION WEBS

By Aldie E. Johnson, Jr.

Langley Aeronautical Laboratory
Langley Field, Va.



Washington

August 1954

AFMDC

TECHNICAL NOTE



NATIONAL ADVISORY COMMITTEE FOR AERONAUTICS

TECHNICAL NOTE 3231

BENDING TESTS ON BOX BEAMS HAVING SOLID- AND

OPEN-CONSTRUCTION WEBS

By Aldie E. Johnson, Jr.

SUMMARY

The results of an exploratory experimental investigation of the effects of replacing alternate webs in a multiweb beam by open, post-stringer construction are reported. Post-stringer (either upright or inclined posts) construction is shown to perform the function of comparable-weight, solid, fabricated webs in the stabilization of the compression cover of a beam in bending both before and after buckling.

INTRODUCTION

The desire to simplify the construction of thin multiweb wings has prompted studies of other lightweight interior structures which alleviate fabrication difficulties with little or no increase in weight or loss of strength. The replacement of alternate solid webs with more open construction, such as longitudinal stringers either alone or connected by upright members, is one method of simplifying the construction of these wings. (See refs. 1, 2, and 3.) An investigation was made to determine whether this method of interior construction could be used to strengthen and stabilize adequately the cover skins of multiweb wings.

This paper presents the results of an exploratory investigation of the buckling strength and after-buckling behavior of several two-cell beams loaded in bending and having covers supported by various forms of internal construction. Two of the beams had a solid internal web and five had open construction; also included was one beam with no internal support. Each of the constructions tested is evaluated in terms of two characteristics: namely, the ability of the internal construction to stabilize the cover skin against buckling and the ability to resist after-buckling distortions of the cover. The proportions of the beams provided a severe test of the latter characteristic because of the large potential margin between buckling and failing moments.

SYMBOLS

A_{sup}	average area of support, $\frac{\text{Total volume of support}}{\text{Total length of support}}$, in. ²
b_S	half of width of beam between center lines of exterior webs, in.
b_W	depth of beam between center lines of covers, in.
c	$c = \frac{b_W + t_S}{2}$
E	modulus of elasticity, ksi
I	moment of inertia of beam, in. ⁴
I_{sup}	moment of inertia of center-line support, in. ⁴
I_t	moment of inertia of rectangular tube, in. ⁴
k_C	plate buckling coefficient for compression cover
l	longitudinal distance between posts, in.
L	beam length exclusive of end attachment, in.
M	experimental moment on beam, in.-kips
M_{cr}	experimental buckling moment, in.-kips
M_f	experimental maximum moment, in.-kips
t_S	average thickness of cover skin, in.
t_W	average thickness of web sheet, in.
β	post spacing ratio, l/b_S
μ	Poisson's ratio
σ_{cr}	calculated average extreme-fiber buckling stress, ksi

σ_{crexp}	experimental average extreme-fiber buckling stress, ksi
σ_{fexp}	experimental modulus of rupture, ksi
T	post-stringer deflectional-stiffness parameter
ψ	effective deflectional stiffness of support, lb/in./in.

DESCRIPTION OF BEAMS

Eight beams, fabricated from a section of drawn 14S-T6 aluminum-alloy rectangular-cross-section tubing with nominal dimensions, as shown in figure 1, were tested in pure bending. A compressive stress-strain curve typical of the tubing material is given in figure 2.

The first beam consisted of an unmodified section of the rectangular tubing and was tested for comparison with the test results for the remaining seven beams which had various forms of internal structure fabricated from 75S-T6 aluminum alloy. The internal structure of these seven beams is illustrated in figure 3. Beams A and B, shown in figures 3(a) and 3(b), had solid webs representing those used in conventional multiweb beam structures. Beam C, shown in figure 3(c), had deep extruded Z-section longitudinal stringers riveted to the center line of each cover. In order to determine the effect of connecting longitudinal stringers by vertical posts at various spacings, beams D, E, and F, shown in figures 3(d), 3(e), and 3(f), were tested. The Z-section stringers used in these beams were shallower than those in beam C. The angle-section posts had a longitudinal spacing corresponding to 2, 1, and 1/2 times the half width of the beam cover. In beam G, figure 3(g), the post members were inclined to form a Warren truss, which gave a structure capable of carrying vertical shear loads.

The weight of the internal structures in the beams was approximately the same with the exception of the structure of beam A which weighed approximately 25 percent more. The supports in all beams were positioned so that the center line of the tubing was midway between the rivet center line and the upright portion of the web or stringer. The supports in beams A, B, and C were riveted to the covers with solid-aluminum flat-head aircraft rivets, and the supports in beams D, E, F, and G were riveted to the covers with Huck blind rivets. All riveting of supports to covers was with 3/16-inch-diameter rivets at 9/16-inch pitch and as close as possible to the web or to the web of the stringer. The detail dimensions and properties of the beams are listed in table I and in figure 3.

TEST PROCEDURE

The beams were loaded to failure in pure bending in the combined load testing machine of the Langley structures research laboratory. Strains were measured at several locations on the beam with Baldwin SR-4 resistance-type wire strain gages, and continuous moment-strain records were obtained during each test. Wire strain gages (type A-9) at the four outside corners of each beam were used to measure the extreme-fiber tensile and compressive strains. An array of wire gages on the compression cover along the center of each bay was used to determine the onset of cover instability due to buckling or wrinkling and also as an indication of the local deformations after buckling. The axial strains in the posts and truss diagonals and the longitudinal strains at the center of each bay on the tension cover were also recorded to give a more complete strain history of the beams and to provide information on the stresses in those regions. Visual observations of the beams under load confirmed the buckling and after-buckling behavior of the beams indicated by the continuously recorded moment-strain data.

RESULTS

One measure of the effectiveness of the internal structure in a multicell beam is its ability to form longitudinal nodes in the compression cover skin at the initiation of cover buckling. In addition, the structure must resist deformation of the cover along the support line in the after-buckling range of loading if a high ultimate strength is to be obtained. The ability of any internal structure to resist after-buckling deformation depends, in part, on the stress level at which buckling of the cover takes place. The beams with a center-line support had a ratio of bay width to skin thickness b_s/t_s equal to 40; thus, buckling of the cover may be anticipated at a relatively low compressive stress. Because of the large potential margin between the buckling stress and the failing stress, the beams in this investigation provided a rather severe test of the resistance of the supports to after-buckling deformations.

Analysis of Buckling Stresses

A theoretical buckling stress for the compressive covers of the beams tested can be determined from the known stability characteristics of similar idealized structures. Charts relating cover-skin stability and support stiffness are given in reference 4 for continuous-line supports and in reference 5 for post-stringer and truss supports. In order to use these charts, the deflectional and rotational stiffnesses of the supports must be evaluated. An experimental method for evaluating the deflectional stiffness of supports is given in reference 5 and this method was used for the test beams. Values of the deflectional stiffness per unit of support length are given in table I for the beams. The design charts of

references 4 and 5 indicate that the deflectional stiffness of the support configurations used in beams A to G is more than adequate to force a line of zero deflection (longitudinal node) over the supporting structure when the cover buckles.

In order to evaluate the effect on the cover buckling stress of the rotational edge restraint provided by the side walls of the beam, the behavior of idealized rectangular-cross-section tubes in bending was used as a guide. The theoretical buckling stress coefficients k_G for a rectangular-cross-section tube having flat walls and right-angle corners (approximated by the tubes used in this investigation) are given in figure 14 of reference 6. For the proportions of the tubes tested, $k_G = 5.5$, which corresponds to an average cover stress at buckling of

$$\sigma_{cr} = \frac{k_G \pi^2 E}{12(1 - \mu^2)} \left(\frac{t_s}{2b_s} \right)^2 = \frac{(5.5)(3.14)^2(10.6)(10^3)(0.123)^2}{12[1 - (0.32)^2](10.056)^2} = 7.98 \text{ ksi}$$

A buckling-stress value of this magnitude may be anticipated for the rectangular-tube specimen without internal structure.

If, as in beams A to G, a line of zero deflection can be assumed to form along the center line of the compression cover of the tube at buckling, a buckling stress coefficient can be determined by using the principles of moment distribution. (See ref. 7.) This calculation yields $k_G = 4.65$ for each bay of the compression cover. A buckling stress coefficient of this magnitude may therefore be anticipated for the beams with internal structure. The predicted stress values based on the actual beam dimensions are listed in table II.

Description of Beam Behavior

The buckling stress for all tests of the present investigation was taken as the elementary beam bending stress M_c/I at which a strain reversal occurred. (See strain-reversal method of ref. 8.) Inasmuch as the walls of the drawn tubing contained initial eccentricities, the buckling stress determined by strain reversal may be anticipated to be somewhat lower than the buckling stress predicted from the theories for initially flat plates. The modulus of rupture (or failing stress) was determined as the M_c/I stress in the covers of the beam when the bending moment was a maximum.

The moment-strain relations at the outside corners of each beam are shown in figure 4. The curves labeled compression give the average strain from the two wire gages at the outside corners on the compression cover

and, correspondingly, the curves labeled tension give the average strain at the outside corners on the tension cover. The maximum moment (shown in table II) carried by each beam is shown by the height of the curves, and the moment at buckling is indicated by the short dashed line through the curves. A description of the experimental behavior of each test beam follows.

Rectangular-tube beam.- As the one-cell beam was loaded, buckling occurred in a regular pattern having half-wave length of buckles of about 75 percent of the cover width. The moment on the beam at which buckling occurred corresponded to an M_c/I stress of about 6.4 ksi. After the compression cover buckled, the buckles grew in magnitude as the loading progressed. A slight shifting of the buckle pattern was noted with no appreciable change in wave length or shape. Failure occurred in an up buckle and an adjacent down buckle at the center of the test section. The modulus of rupture of the beam was 31.2 ksi. The corners of the beam remained straight (except for curvature of the beam due to bending) until failure when they crimped slightly.

Beam A.- Beam A had the highest experimental buckling stress and modulus of rupture of the beams tested. Although the web was slightly heavier than the supports used in the remaining beams, beam A can be used as a basis of comparison of the strengths of the remaining beams. Local buckling of the compression cover occurred at a cover stress of about 27.6 ksi (which corresponds to $k_c = 4.7$ based on the cover half width b_g) in a very regular pattern with a longitudinal node forming over the center web. As the loading of the beam progressed, the magnitude of the buckles in the compression cover increased slowly until failure occurred near one end of the test section at a modulus of rupture of 42.0 ksi. The center support maintained a longitudinal node in the cover until, at failure, the attachment flange of the angle cap tore away from the leg attached to the web and allowed the cover to fail in an up buckle across the entire beam. There were no rivet failures.

Beam B.- The channel-type web used in beam B was formed from aluminum-alloy-sheet material - a method of fabricating webs somewhat simpler than riveting a sheet to web-cap members as in the web of beam A. The cover of beam B buckled locally at an M_c/I stress of 26.9 ksi with a longitudinal node evident along the center web. The buckle pattern was not as regular as in beam A, however, and, at a cover stress of approximately 29.0 ksi, deflection of the cover over the web line was observed both visually and on the moment-strain records. The buckles on either side of the web shifted slightly so that up buckles tended to join over the web and formed a series of skewed wave crests with respect to the axis of the beam. This "washboard" pattern developed gradually along the beam and with increasing distortion of the support line. Failure occurred at a modulus of rupture of 35.6 ksi in a down trough across the beam. The corner of the center web crimped as the cover failed, but the corners of the exterior webs remained straight.

Beam C.- Beam C, which was stiffened by deep longitudinal Z-section stringers, showed a behavior different from that of the previous beams in that, as the loading was applied, dishing of the covers took place between exterior webs. The dishing caused a buildup of stress at the corners of the beam (evident from the moment-strain curves of fig. 4). The compression cover behaved as a stiffened plate with supported side edges, with buckling occurring in one-half wave in the test length. At a load of approximately two-thirds of the ultimate load on the beam, a superimposed local buckling of the compression cover took place with a node along the stringer. As the ultimate load on the specimen was reached, dishing of the cross section grew in magnitude with an accompanying drop in load. The maximum load on the beam corresponded to a modulus of rupture of 39.2 ksi.

Beam D.- In the test of beam D (which had the largest spacing between posts), local buckling of the compression cover occurred at an M_c/I stress of 21.4 ksi in a somewhat irregular pattern. Shortly after initial buckling, the buckles tended to join across the stringer; as a result there was bending of the stringer and a skewed buckle pattern was created. This pattern is evident in figure 5 which shows the deformation of the cover along the rivet line. These distortions increased in magnitude until failure occurred in a down buckle at the midsection of the beam (between posts). Local bending of the stringer was appreciable, and the attachment flange of the stringer tore away from the stringer web. A few blind rivets failed in tension in the up buckle over the post to the right of the failure trough. (See fig. 6.) The modulus of rupture was 36.8 ksi. No overall dishing of the covers was evident.

Beam E.- Local buckling of beam E (which had intermediate spacing between posts) occurred at an M_c/I stress of 22.2 ksi in a regular pattern with a longitudinal node forming over the center support. Figure 7 shows a picture of the beam shortly after buckling. The strain-gage lead wires have been removed so that the buckles are more easily seen. Prior to failure of the beam, the buckle pattern shifted to the form with transverse nodes across the entire compression cover. The nodes corresponded approximately to the post locations, an indication that deflections of the compression stringer and cover took place mainly in the regions between posts. These deflections are evident in figure 8. Failure occurred at a modulus of rupture of 38.1 ksi near one end of the test section when the blind rivets failed in tension as an up buckle tried to form over a post.

Beam F.- Buckling of beam F (which had the smallest spacing between posts) occurred at an M_c/I stress of 23.4 ksi in a regular pattern with a longitudinal node forming over the center support. Figure 9 shows a picture of the beam in the range beyond buckling. The lead wires from the wire strain gages have been removed from the beam so that the buckle pattern is more easily seen (for this reason the compression curve for

beam F in fig. 4 is incomplete). The locations of the posts are indicated by marks along the line of rivets. The longitudinal node remained along the support line until failure occurred at one end of the test section in an up buckle across the beam. The blind rivets failed in tension and, as in the failure of beams A and D, the attachment flange of the stringer tore apart from the web of the stringer. Severe distortions of the stringer were evident at the post locations near the point of failure. The modulus of rupture was 41.4 ksi.

Beam G. - At an M_c/I stress of 23.6 ksi, the compression cover of beam G (which was stiffened internally with a Warren truss) buckled locally in a regular pattern with the truss support maintaining a longitudinal node. As the loading progressed, buckles on either side of the stringer joined together over a panel point of the truss; this caused appreciable tensile forces in the blind rivets and consequently failure of the rivets and the beam. The modulus of rupture was 38.8 ksi. Strain readings on the diagonal members of the truss indicated very small loads in those members at failure. Inspection of the support after testing showed that the diagonals and stringers were adequately riveted together and the truss members relatively undeformed. The failure of the beam may have been premature because of the tensile failure of the blind rivets on the cover.

DISCUSSION

The buckling and failing moments and stresses for each beam are tabulated in table II. For comparison purposes, the buckling and failing stresses of the beams are also shown in a bar graph, figure 10. The sketch above each bar indicates the construction of the center support. Because of the different mode of instability and failure in beam C, the results for this beam are not shown on the bar graph. The moduli of rupture of the beams are shown by the height of the bars, and the experimental buckling stresses for the beams are shown by the height of the shaded portion of the bars. The predicted cover buckling stress for each beam is indicated by the short dashed lines on either side of the bar. The agreement between the experimentally determined and predicted buckling stresses is considered satisfactory in view of the initial waviness of the walls of the drawn tubes.

The advantage of high local stiffness of attachment of the web to the compression cover is illustrated by the increase in strength of beam A over beam B. In beam A the rivet line on the attachment flange was closer to the web plane than in beam B which, in combination with the square corner on the attachment angle, greatly increases the deflectional stiffness of the web construction (see table I).

The experiments with the post-stringer type of support indicate that an open structure can provide a deflectional support to the covers comparable to that provided by solid webs. In order to maintain continuity of supports in the after-buckling range of loading, the bending stiffness of the stringers between posts should be substantially greater than the minimum stiffness required to form a longitudinal node at the initiation of buckling. This stiffness may be achieved by using posts at a fairly small spacing, as illustrated by beam F, or by increasing the moment of inertia of the stringer. The slight increase in beam buckling stress between beams D and F may be attributed to the improved torsional stiffness of the longitudinal stringer when restrained by posts at a small spacing.

The performance of beam G with the Warren truss indicates that, with a given longitudinal stringer, this type of structure provides a support to the compression cover comparable to that provided by vertical posts at a spacing somewhat less than the spacing of the panel points of the truss.

The severity of cross-sectional dishing that occurred with longitudinal stringers in beam C would not be anticipated in a multicell beam because of the restraint offered by adjacent cells. The test indicates, however, the type of distortion that may occur in a long plate with a single longitudinal stringer when the stringer is supported at infrequent intervals by either ribs or posts.

CONCLUDING REMARKS

The results of an experimental investigation of the buckling strength and after-buckling behavior of several two-cell beams indicate that open construction utilizing post-stringer or truss supports can perform the function of a solid web in stabilizing the covers of a beam in bending with no increase in weight over a solid web.

The tests indicate that the following factors contribute toward improving the efficiency of alternate webs in a multiweb beam:

- (1) high local cross-sectional stiffness of flange attaching support to cover skins
- (2) provision of adequate bending stiffness in the stringers of post-stringer beams in order to resist after-buckling distortions of the cover skins
- (3) torsional restraint along the support line to raise the buckling stress to its maximum.

The highest buckling and maximum strengths of the beams tested were noted in the beam which had the highest combination of torsional and deflectional stiffnesses.

Langley Aeronautical Laboratory,
National Advisory Committee for Aeronautics,
Langley Field, Va., June 3, 1954.

REFERENCES

1. Barrett, Paul F., and Seide, Paul: An Experimental Determination of the Critical Bending Moment of a Box Beam Stiffened by Posts. NACA TN 2414, 1951.
2. Badger, D. M.: Analysis and Design of Multipost-Stiffened Wings. Aero. Eng. Rev., vol. 12, no. 7, July 1953, pp. 45-57.
3. Anderson, Roger A., Pride, Richard A., and Johnson, Aldie E., Jr.: Some Information on the Strength of Thick-Skin Wings With Multiweb and Multipost Stabilization. NACA RM L53F16, 1953.
4. Anderson, Roger A., and Semonian, Joseph W.: Charts Relating the Compressive Buckling Stress of Longitudinally Supported Plates to the Effective Deflectional and Rotational Stiffness of the Supports. NACA TN 2987, 1953.
5. Anderson, Roger A., Johnson, Aldie E., Jr., and Wilder, Thomas W., III: Design Data for Multipost-Stiffened Wings in Bending. NACA TN 3118, 1954.
6. Anderson, Roger A.: Some Preliminary Information on Buckling and Ultimate Strength of Unstiffened Compression Skin Obtained Through Bending and Compression Tests on Rectangular Cross Section Aluminum Tubes. Rep. No. 27, Aero. Res. Inst. of Sweden (Stockholm), 1949.
7. Lundquist, Eugene E., Stowell, Elbridge Z., and Schuette, Evan H.: Principles of Moment Distribution Applied to Stability of Structures Composed of Bars or Plates. NACA Rep. 809, 1945. (Formerly NACA ARR 3K06.)
8. Hu, Pai C., Lundquist, Eugene E., and Batdorf, S. B.: Effect of Small Deviations From Flatness on Effective Width and Buckling of Plates in Compression. NACA TN 1124, 1946.

TABLE I.- PROPERTIES OF BEAMS

14S-76 drawn-aluminum tubing
738-76 aluminum supports

Beam	t_g , in.	t_w , in.	b_g , in.	b_g/t_g	b_w/b_g	l , in.	β (Nominal)	L , in.	Post, in. (a)	A_{sup} , in. ²	I , in. ⁴	I_{sup} , in. ⁴	$\frac{1}{2}$ lb/in./in. (tension)	$\frac{1}{2}$ lb/in./in. (compression)	T	Riveting		
																Stringer to cover	Web to stringer	Post to stringer
Rectangu- lar tube	0.123		5.03	41.8	0.507			31.56			18.791							
A	.123	0.051	5.04	41.0	1.018			32.56		0.400	20.133	1.253	13,000	12,500		AN442AD-6-7 at 9/16 pitch	AN442AD-3-3 at 3/16 pitch	
B	.122	.051	5.02	41.2	1.019			41.56		.516	19.773	.970	3,300	3,130		AN442AD-6-7 at 9/16 pitch		
C	.121		5.03	41.5	1.016			29.06		.324	20.107	1.583				AN442AD-6-7 at 9/16 pitch		
D	.121		5.07	41.9	1.018	10.0	2	39.73	$\frac{1}{8} \times .90 \times .90$.519	20.393	1.333	2,430	6,540	1.87	^c AN456, 3/16 diam at 9/16 pitch		AN442AD-8-8
E	.121		5.03	41.7	1.022	5.0	1	39.73	$\frac{1}{16} \times .85 \times .85$.514	20.397	1.330	4,530	10,600	3.44	^c AN456, 3/16 diam at 9/16 pitch		AN442AD-6-6
F	.121		5.07	41.9	1.018	2.5	$\frac{1}{2}$	39.73	$\frac{1}{16} \times \frac{1}{2} \times \frac{3}{8}$.517	20.386	1.334	5,920	14,600	4.52	^c AN456, 3/16 diam at 9/16 pitch		AN442AD-6-6
G	.121		5.07	41.9	1.014	9.375	$\frac{15}{8}$	40.62	$\frac{1}{16} \times \frac{3}{8} \times \frac{5}{8}$.322	20.174	1.289	1,830	3,320	1.41	^c AN456, 3/16 diam at 9/16 pitch		AN442AD-8-8

^aPosts and truss diagonals are angle sections.

^bValue represents $2b_g/t_g$.

^cUse blind rivets.

TABLE II.- TEST DATA FOR BEAMS

Beam	M_{cr} , in.-kips	M_f , in.-kips	σ_{crexp} , ksi	σ_{fexp} , ksi	σ_{cr} , ksi
Rectangular tube	46	225	6.39	31.2	7.98
A	213	324	27.6	42.0	26.9
B	203	269	26.9	35.6	26.6
C		301		39.2	26.2
D	165	284	21.4	36.8	25.7
E	171	294	22.2	38.1	25.9
F	181	320	23.4	41.4	25.7
G	181	298	23.6	38.8	25.7

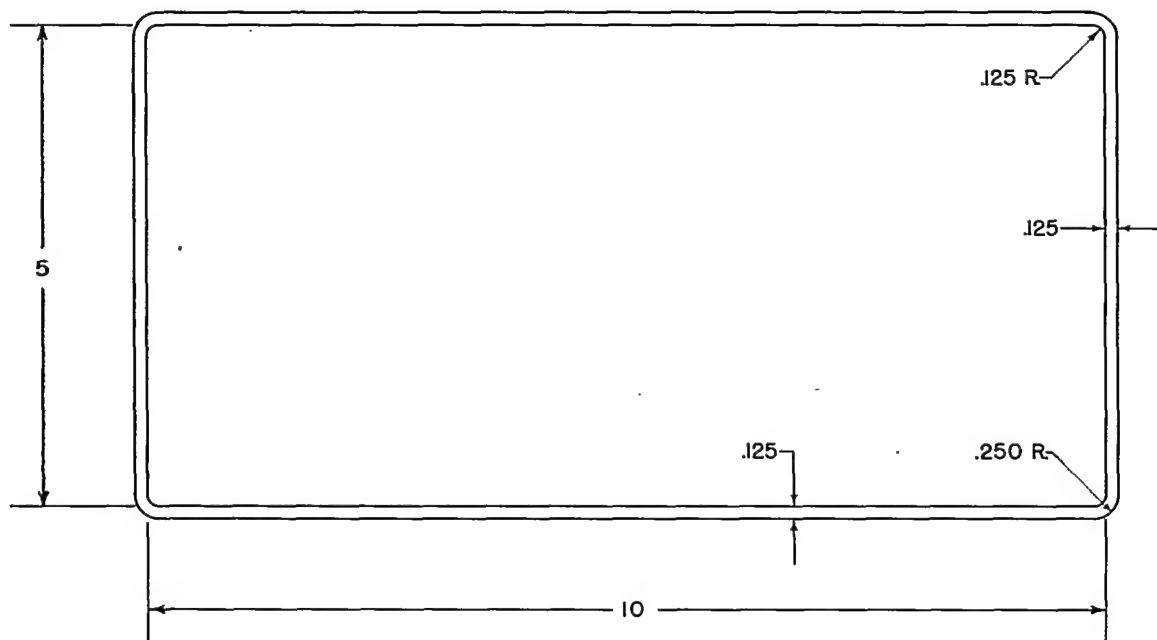


Figure 1.—Nominal dimensions of rectangular tubing used in beams.

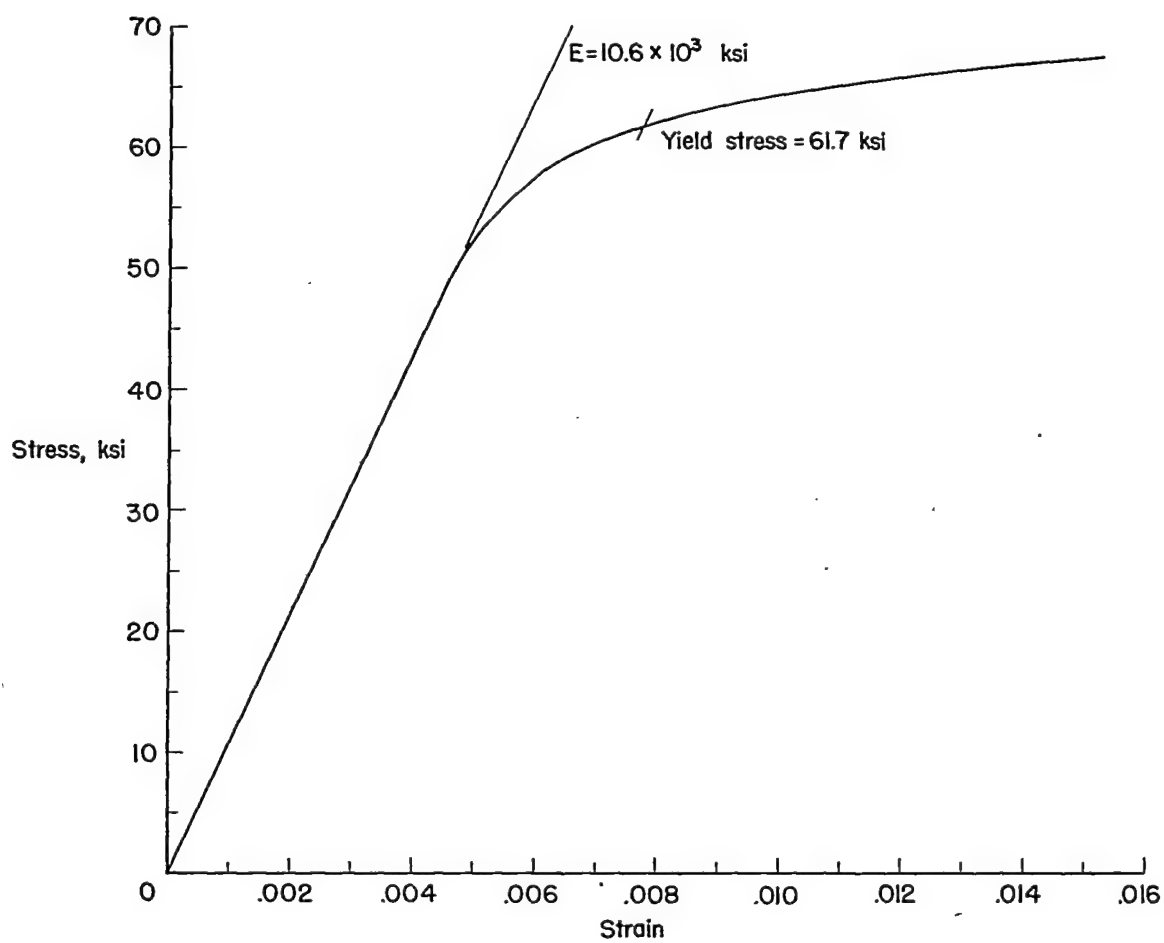
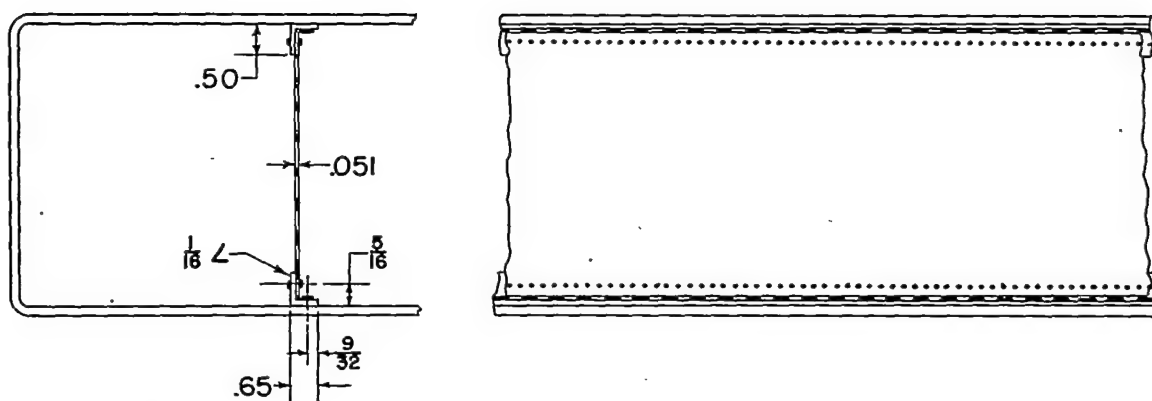
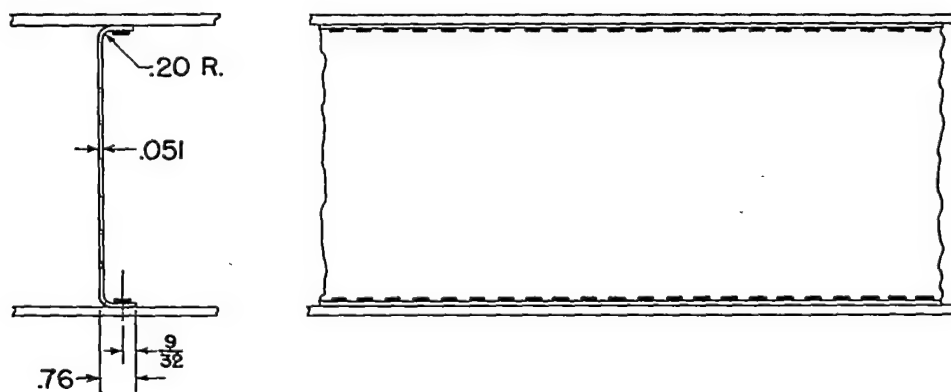


Figure 2.—Typical compressive stress-strain curve for 14S-T6 aluminum alloy.

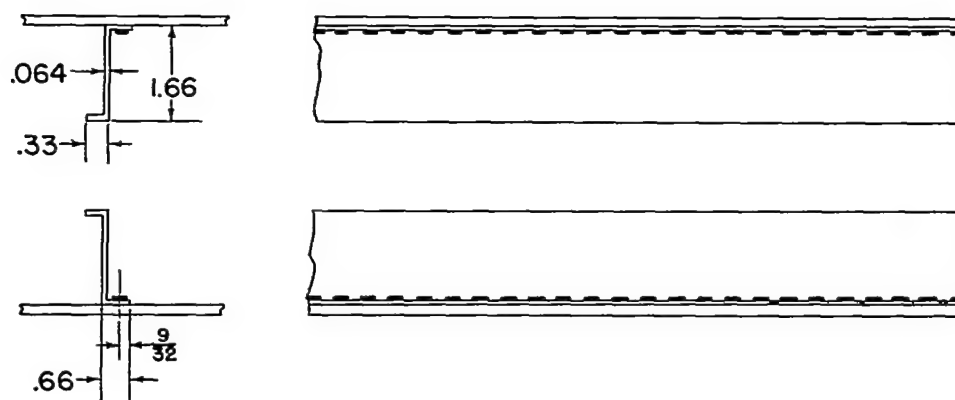


(a) Fabricated web (0.051 inch thick) with extruded angle caps. Beam A.



(b) Formed channel web (0.051 inch thick). Beam B.

Figure 3.—Supporting structure along center line of two-cell beams.



(c) Z-stringer construction. Beam C.

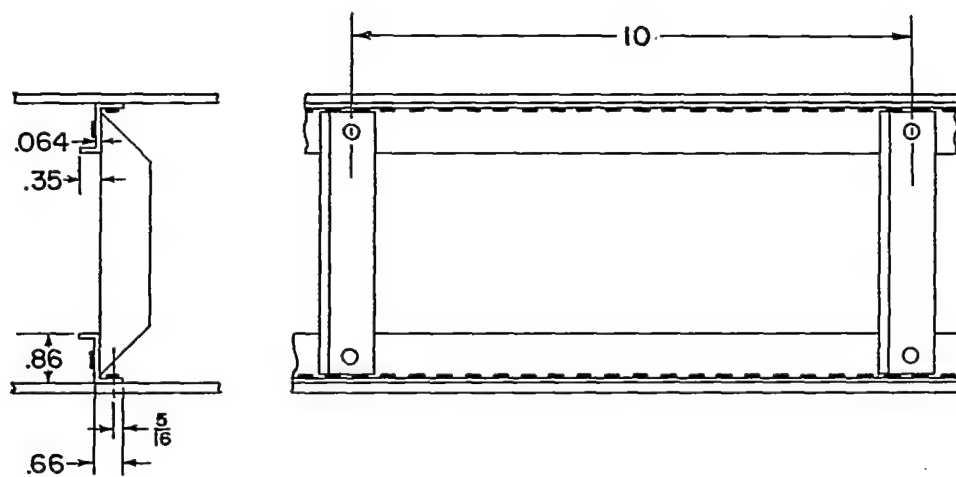
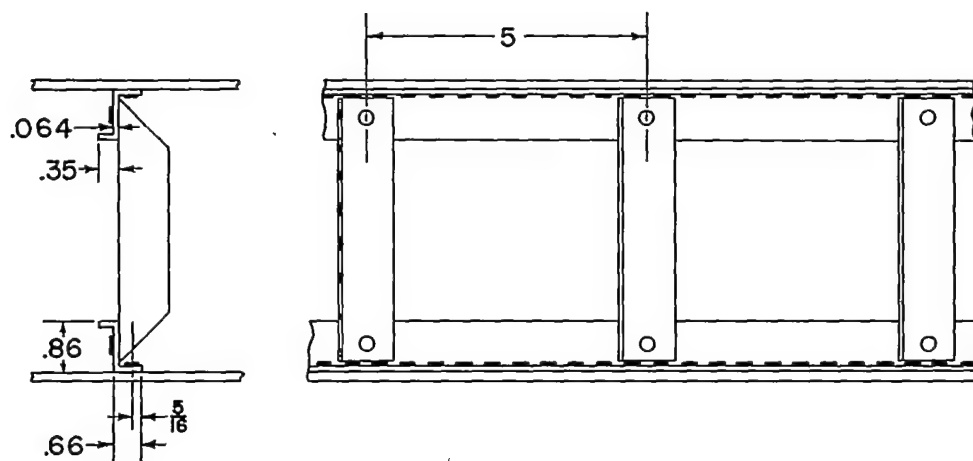
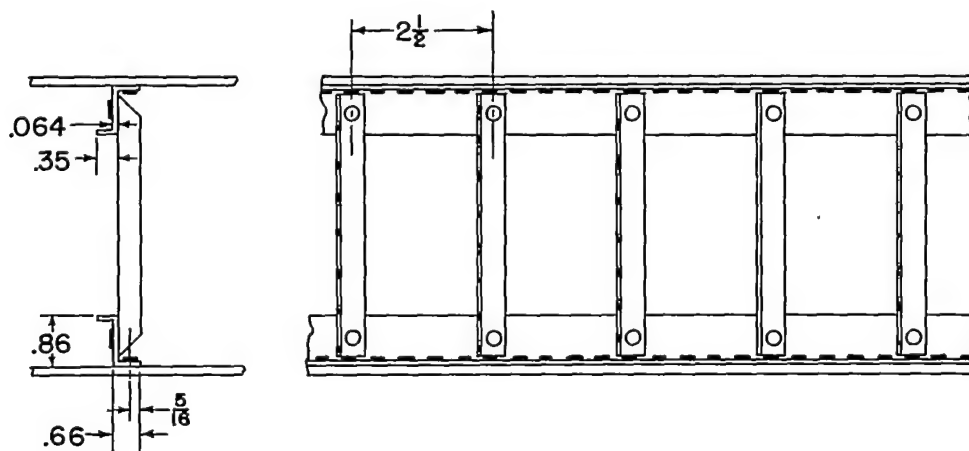
(d) $\beta=2$ post-stringer construction. Beam D.

Figure 3.—Continued.

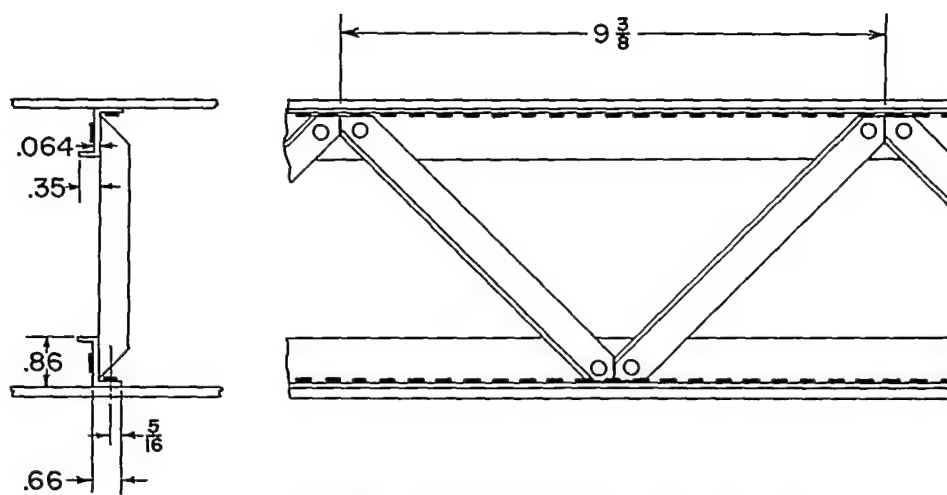


(e) $\beta = 1$ post-stringer construction. Beam E.



(f) $\beta = \frac{1}{2}$ post-stringer construction. Beam F.

Figure 3.-Continued.



(g) Warren truss construction. Beam G.

Figure 3.—Concluded.

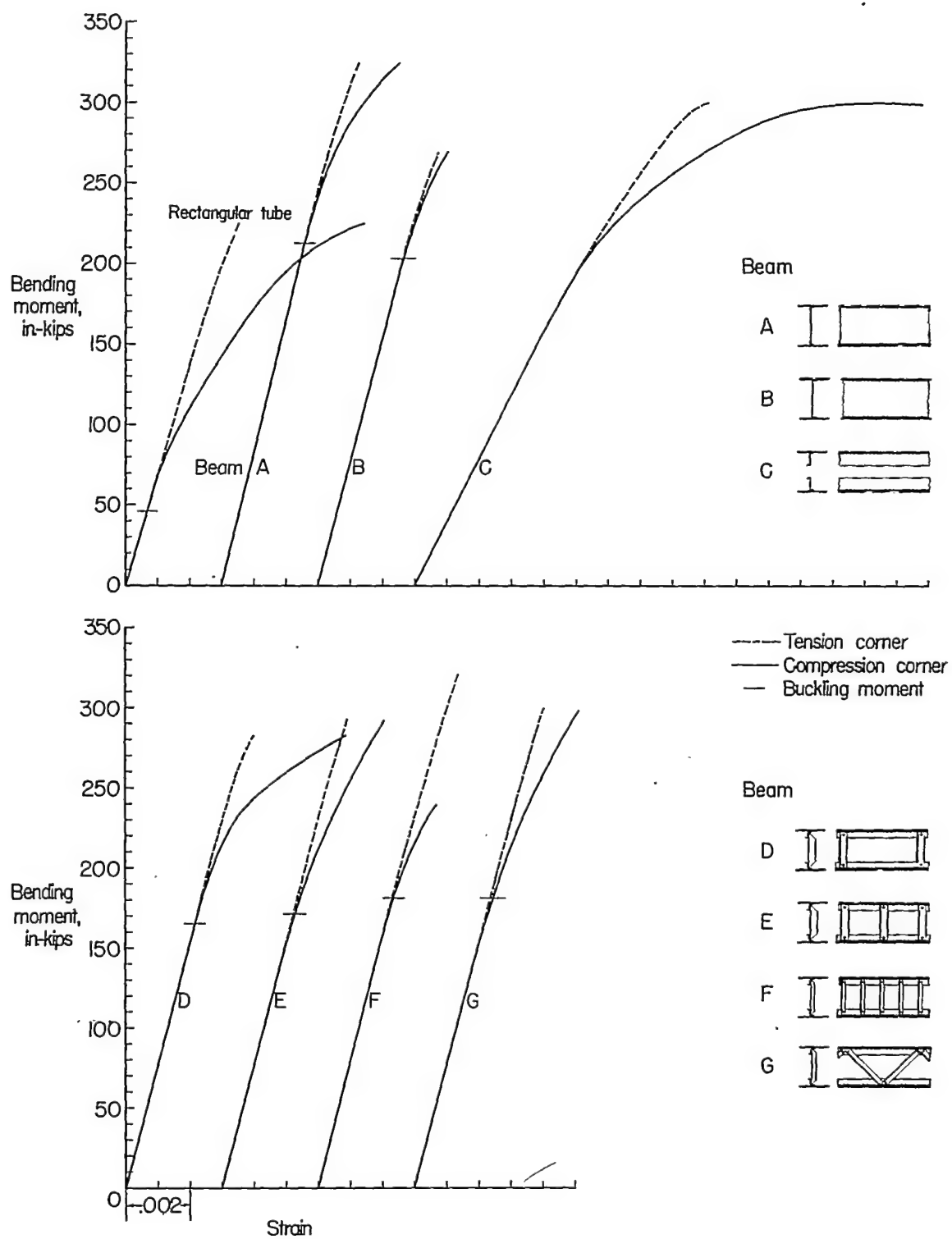
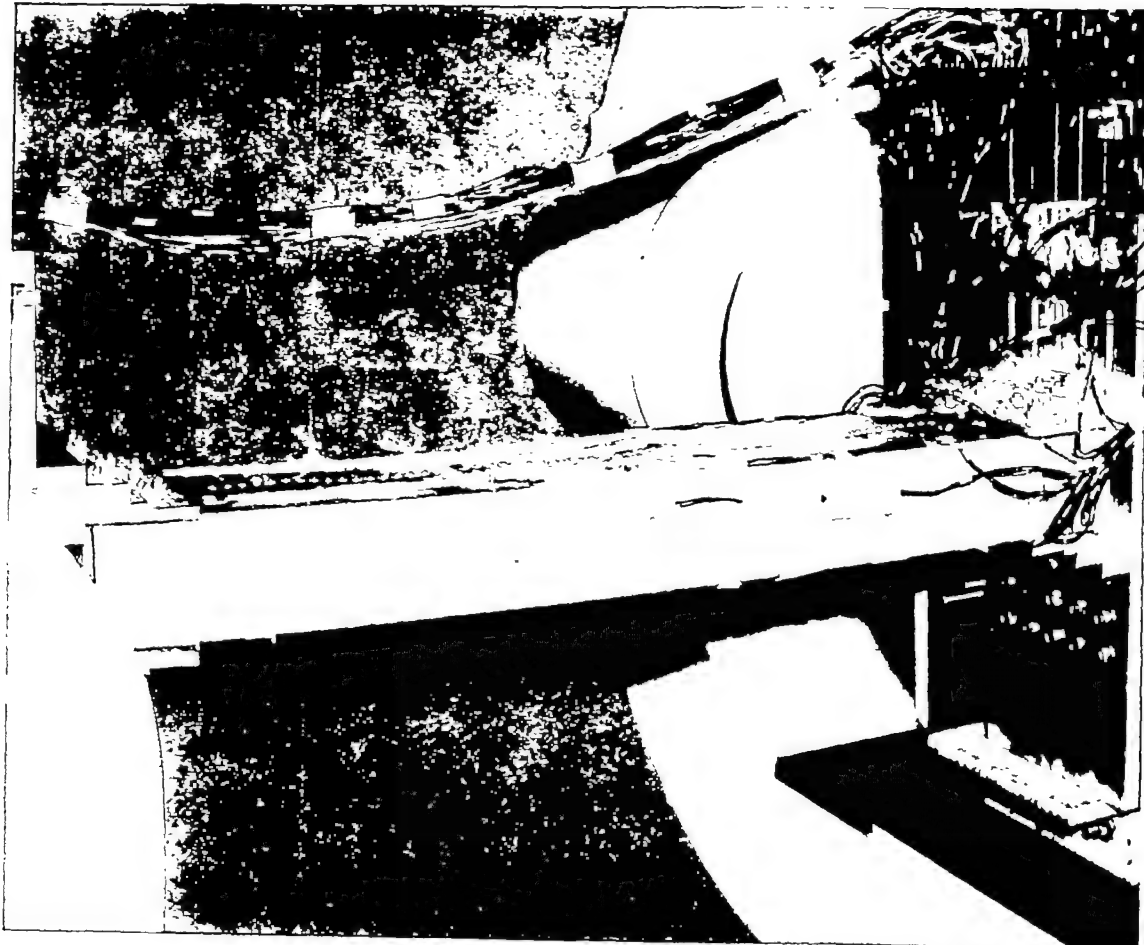
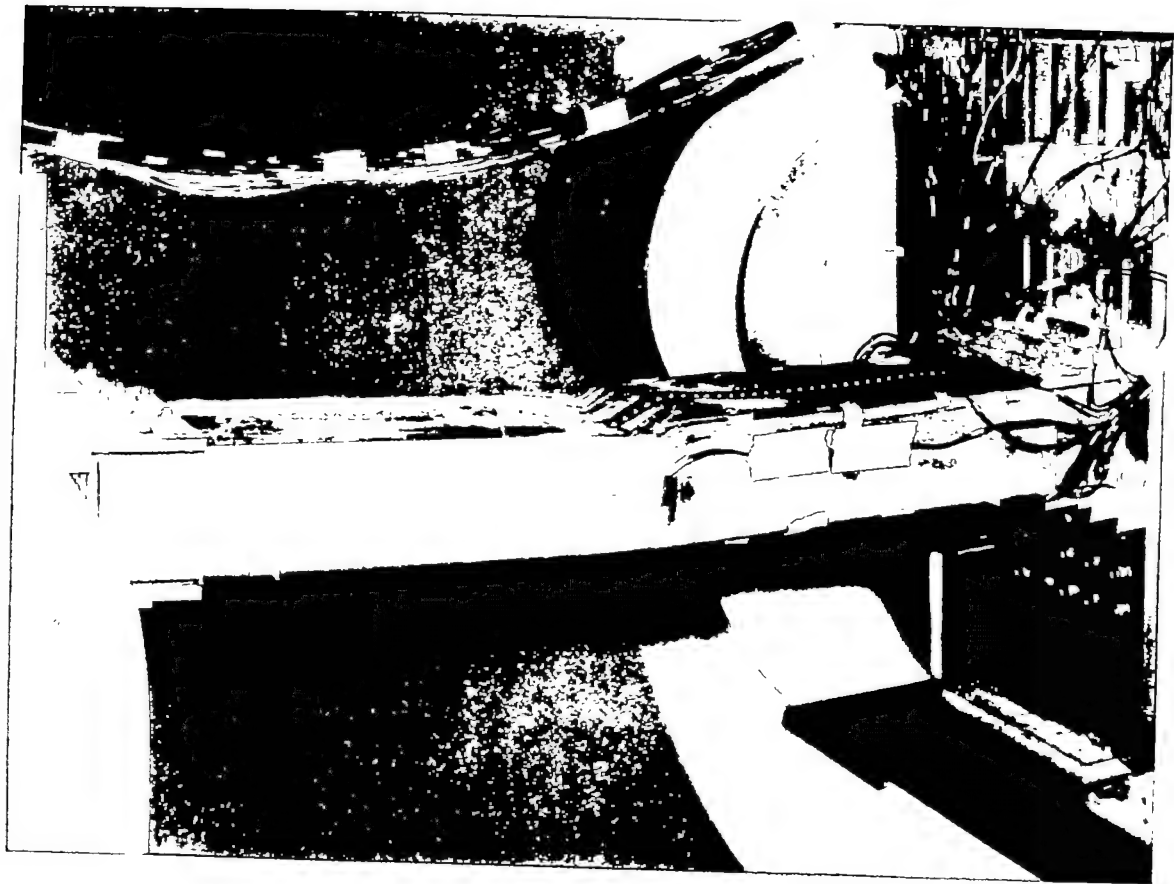


Figure 4.—Moment-strain relations at outside corners of beams in bending.



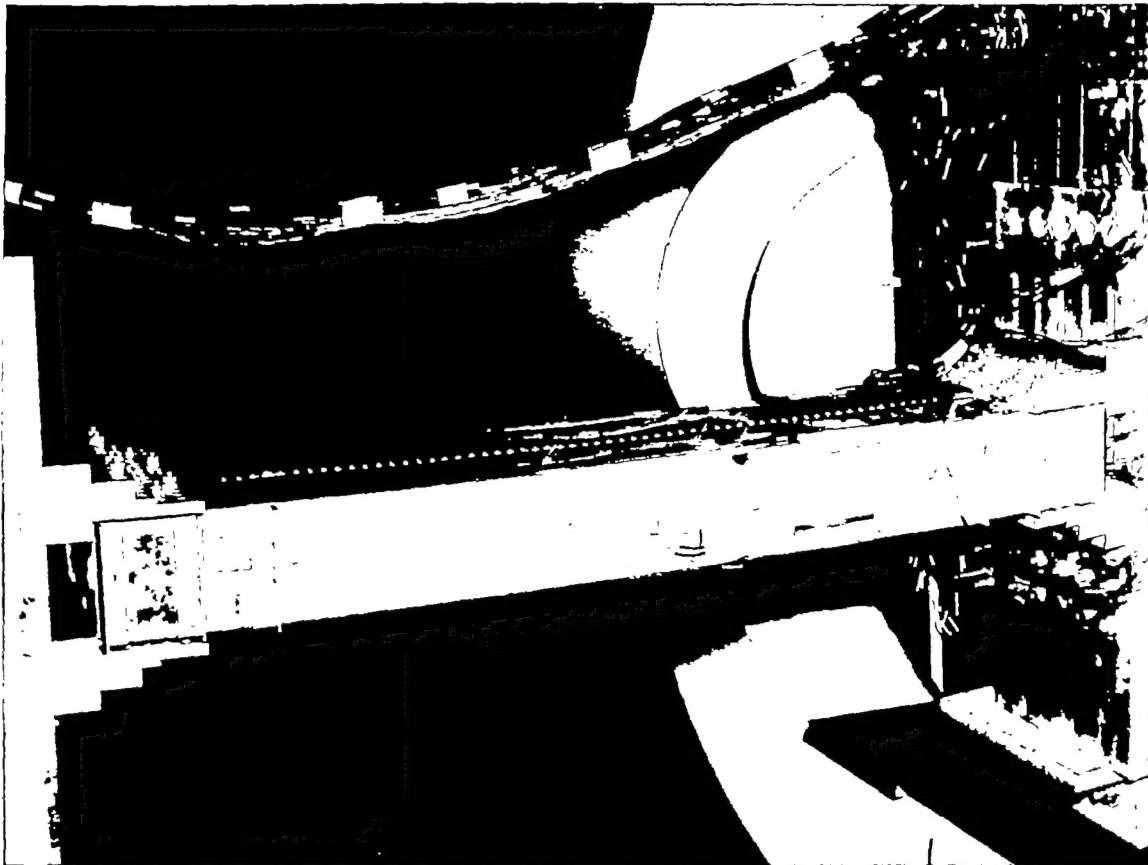
77824.1

Figure 5.—Beam D showing buckle pattern with skewed transverse nodes in top cover.



77825.1

Figure 6.—Beam D after failure.



77826.1

Figure 7.—Beam E shortly after buckling with longitudinal node and local buckles showing in top cover.



77827.1

Figure 8.—Beam E prior to failure with transverse nodes and "washboard" pattern of buckles showing in top cover.



77796.1

Figure 9.—Beam F showing longitudinal node along center of top cover and local buckles in cover.

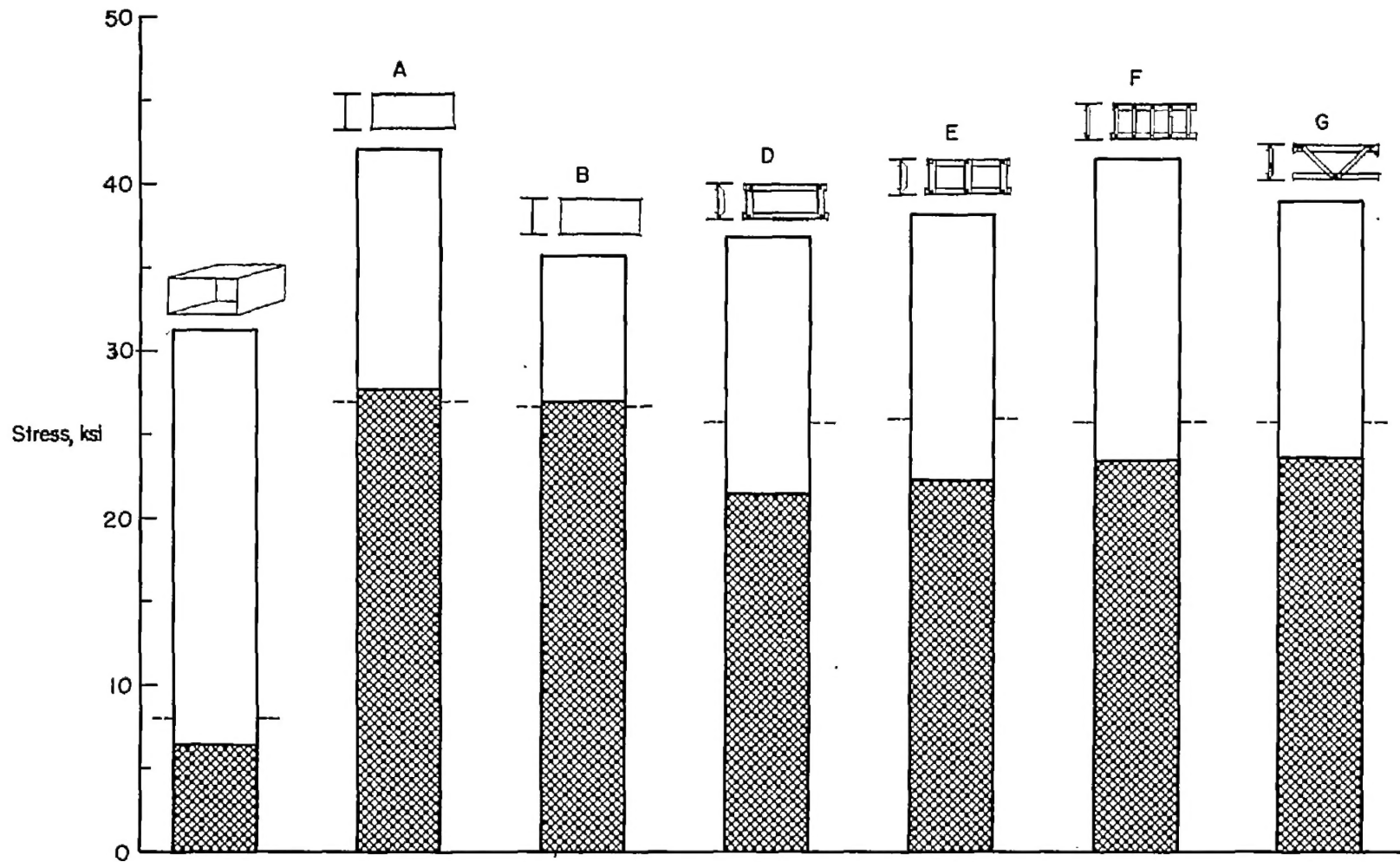


Figure 10.-Comparative bending strengths of two-cell beams having various center-line supports.